



# Artificial Neural Networks Approach for the Prediction of Thermal Balance of SI Engine Using Ethanol-Gasoline Blends

Mostafa Kiani Deh Kiani, Barat Ghobadian, Fathollah Ommi, Gholamhassan Najafi, Talal Yusaf

## ► To cite this version:

Mostafa Kiani Deh Kiani, Barat Ghobadian, Fathollah Ommi, Gholamhassan Najafi, Talal Yusaf. Artificial Neural Networks Approach for the Prediction of Thermal Balance of SI Engine Using Ethanol-Gasoline Blends. Gerald Quirchmayr; Josef Basl; Ilsun You; Lida Xu; Edgar Weippl. International Cross-Domain Conference and Workshop on Availability, Reliability, and Security (CD-ARES), Aug 2012, Prague, Czech Republic. Springer, Lecture Notes in Computer Science, LNCS-7465, pp.31-43, 2012, Multidisciplinary Research and Practice for Information Systems. .

**HAL Id: hal-01542472**

**<https://hal.inria.fr/hal-01542472>**

Submitted on 19 Jun 2017

**HAL** is a multi-disciplinary open access archive for the deposit and dissemination of scientific research documents, whether they are published or not. The documents may come from teaching and research institutions in France or abroad, or from public or private research centers.

L'archive ouverte pluridisciplinaire **HAL**, est destinée au dépôt et à la diffusion de documents scientifiques de niveau recherche, publiés ou non, émanant des établissements d'enseignement et de recherche français ou étrangers, des laboratoires publics ou privés.



Distributed under a Creative Commons Attribution 4.0 International License

# Artificial neural networks approach for the prediction of thermal balance of SI engine using ethanol- gasoline blends

Mostafa Kiani Deh Kiani<sup>1</sup>, Barat Ghobadian<sup>\*1</sup>, Fathollah Ommi<sup>1</sup>, Gholamhassan Najafi<sup>1</sup> and Talal Yusaf<sup>2</sup>

<sup>1</sup>Tarbiat Modares University, Tehran - Iran P.O.Box:14115-111

Corresponding author: Email address: ghobadib@modares.ac.ir  
Tel. /fax: +98 21 44196522.

<sup>2</sup>University of Southern Queensland (USQ) Australia, Toowoomba Campus, Faculty of Engineering and Surveying Mechanical and Mechatronic Engineering, talal.yusaf@usq.edu.au

**Abstract.** This study deals with artificial neural network (ANN) modeling of a spark ignition engine to predict engine thermal balance. To acquire data for training and testing of ANN, a four-cylinder, four-stroke test engine was fuelled with ethanol-gasoline blended fuels with various percentages of ethanol and operated at different engine speeds and loads. The performance of the ANN was validated by comparing the prediction data set with the experimental results. Results showed that the ANN provided the best accuracy in modeling the thermal balance with correlation coefficient equal to 0.997, 0.998, 0.996 and 0.992 for useful work, heat lost through exhaust, heat lost to the cooling water and unaccounted losses respectively. The experimental results showed as the percentage of ethanol in the ethanol-gasoline blends is increased, the percentage of useful work is increased, while the heat lost to cooling water and exhaust are decreased compared to neat gasoline fuel operation.

**Keywords:** SI engine, thermal balance, ethanol-gasoline blends, artificial neural network

## 1 Introduction

Artificial neural networks (ANN) are used to solve a wide variety of problems in science and engineering, particularly for some areas where the conventional modeling methods fail. A well-trained ANN can be used as a predictive model for a specific application, which is a data-processing system inspired by biological neural system. The predictive ability of an ANN results from the training on experimental data and then validation by independent data. An ANN has the ability to re-learn to improve its performance if new data are available [1]. An ANN model can accommodate multiple input variables to predict multiple output variables. It differs from conventional modeling approaches in its ability to learn the system that can be modeled without prior knowledge of the process relationships. The prediction by a well-trained ANN is normally much faster than the conventional simulation programs or mathematical models as no lengthy iterative calculations are needed to solve differential equations using numerical methods but the selection of an appropriate neural network topology is important in terms of model accuracy and model simplicity. In addition, it is possible to add or remove input and output variables in the ANN if it is needed. Some researchers studied this method to predict internal combustion engine characteristics. Najafi and his co-worker [2] used ANNs to predict Performance and exhaust emissions of a gasoline engine. Authors in reference [3] have investigated the effect of cetane number on exhaust emissions from engine with the neural network. Canakci and his co-worker [4] analyzed performance and exhaust emissions of a diesel engine fuelled with biodiesel produced from waste frying palm oil using ANN. The effects of valve-timing in a spark ignition engine on the engine performance and fuel economy was investigated by Golcu et al. [5]. Kalogirou [6] reviewed Artificial intelligence for the modeling and control of combustion processes. A number of AI techniques have been described in this paper. Czarnigowski [7] used neural network model-based observer for idle speed control of ignition in SI engine. References [8–15] investigated the performance of various thermal systems with the aid of ANN. The ANN approach was used to predict the performance and exhaust emissions of internal combustion engines [16-22]. In the existing literatures, it was shown that the use of ANN is a powerful modeling tool that has the ability to identify complex

relationships from input–output data. Therefore, the objective of this study is to develop a neural network model for predicting the thermal balance of the engine in relation to input variables including engine speed, engine load and fuel blends. The thermal balance was respect of useful work, heat lost through exhaust, heat lost to the cooling water and unaccounted losses (i.e. heat lost by lubricating oil, radiation). This model is of a great significance due to its ability to predict thermal balance of engine under varying conditions.

## 2 Data gathering method

In this study, the experiments were performed on a KIA 1.3 SOHC, four-cylinders, four-stroke, and spark ignition (SI) gasoline engine. Specifications of the engine are presented in Table 1. A 190 kW SCHENCK-WT190 eddy-current dynamometer was used in the experiments in order to measure engine brake power. Fuel consumption rate was measured by using laminar type flow meter, Pierburg model. Air consumption was measured using an air flow meter. The temperatures for the various points were recorded using thermocouples. All of the thermocouples were type-K (Cr–Al). Temperature measuring points are presented in Table 2. Five separate fuel tanks were fitted to the gasoline engine and these contained gasoline and the ethanol-gasoline blends. The experimental setup for gathering data is shown in Fig. 1. The thermal balance from the engine running on ethanol- gasoline blends (E0, E5, E10, E15 and E20) were evaluated. All the blends were tested under varying engine speed (1000-5000 rpm with 500 rpm interval) and at constant engine loads of 25, 50, 70% and full load conditions. Properties of fuels used in this research have been indicated in Table 3.

**Table 1.** Technical specifications of the test engine

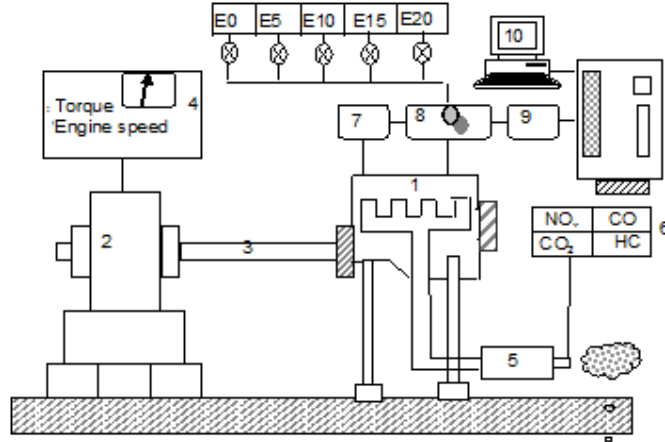
Engine type	SOHC, fuel injected
Number of cylinder	4
Compression ratio	9.7
Bore (mm)	71
Stroke (mm)	83.6
Displacement volume (cc)	1323
Max. power (kW)	64 at 5200 rpm
Cooling system	Water-cooled

**Table 2.** Points of thermocouples

T1	Inlet water to engine
T2	Outlet water from engine
T3	Inlet air
T4	exhaust gases

**Table 3.** Properties of ethanol and gasoline

Fuel property	Ethanol	Gasoline
Formula	C <sub>2</sub> H <sub>5</sub> OH	C <sub>4</sub> to C <sub>12</sub>
Molecular weight	46.07	100-105
Density, g/cm <sup>3</sup> at 20 °C	0.79	0.74
Lower heating value, MJ/kg	25.12	45.26
Stoichiometric air- fuel ratio, Wight	9	14.7
Specific heat, kJ/kg K	2.38	1.99
Heat of vaporize, kJ/kg	839	305



1. Engine; 2.Dynamometer; 3.Drive shaft; 4.Dynamometer control unit, load & speed indicator;  
5.Exhaust; 6.Gas analyzer; 7. Air flow meter; 8.Fuel measurement system; 9.Measuring boom;  
10.Computer

**Fig. 1.** Schematic diagram of experimental setup

The thermal losses through the various points were calculated as follows.

The total heat supplied by the fuel ( $Q_t$ ) was calculated by the following formula:

$$Q_t = \dot{m}_f \cdot CV \quad (1)$$

Where,  $\dot{m}_f$  is the fuel consumption rate (kg/s) and  $CV$  is the lower calorific value of the fuel, (kJ/kg). The useful work ( $P_b$ ) was measured by the dynamometer. The heat rejected to the coolant water ( $Q_w$ ) was determined by:

$$Q_w = \dot{m}_w \cdot C_w \cdot (T_2 - T_1) \quad (2)$$

Where,  $\dot{m}_w$  is the water flow rate (kg/s),  $C_w$  is the specific heat of water (kJ/kg °C),  $T_1$  is the inlet water temperature (°C) and  $T_2$  is the outlet water temperature (°C). The sensible enthalpy loss is considered for the exhaust flow in this study. The heat lost through the exhaust gases ( $Q_e$ ) was calculated considering the heat necessary to increase the temperature of the total mass (fuel + air),  $\dot{m}_e$  (kg/s), from the outside conditions  $T_3$  (°C) to the temperature of the exhaust  $T_4$  (°C). This heat loss is also known as sensible heat, and to calculate it, it is necessary to calculate the mean specific heat of the exhaust gases ( $C_e$ ), which, in this case, is assumed to be the value for air with a mean temperature of the exhaust [23].

$$Q_e = \dot{m}_e \cdot C_e \cdot (T_4 - T_3) \quad (3)$$

The unaccounted heat losses are the heat rejected to the oil plus convection and radiation heat losses from the engine external surfaces. The unaccounted heat losses ( $Q_u$ ) are given as:

$$Q_u = Q_t - (Q_w + Q_e + P_b) \quad (4)$$

### 3 Neural network design

To get the best prediction by the network, several structures were evaluated and trained using the experimental data. Back-propagation is a network created by generalizing the Widrow-Hoff learning rule to multiple-layer networks and nonlinear differentiable transfer functions. Input vectors and the corresponding target vectors are used to train a network until it can approximate a function.

Networks with biases, a sigmoid layer, and a linear output layer are capable of approximating any function with a finite number of discontinuities. Standard back-propagation is a gradient descent algorithm, as is the Widrow-Hoff learning rule, in which the network weights are moved along the negative of the gradient of the performance function. Each neuron computes a weighted sum of its n

input signals,  $x_j$ , for  $j=1, 2, \dots, n$ , and then applies a nonlinear activation function to produce an output signal  $y$ :

$$y = \varphi\left(\sum_{j=1}^n w_j x_j\right) \quad (5)$$

The performance of the network can be evaluated by comparing the error obtained from converged neural network runs and the measured data. Error was calculated at the end of training and testing processes based on the differences between targeted and calculated outputs. The back-propagation algorithm minimizes an error function defined by the average of the sum square difference between the output of each neuron in the output layer and the desired output. The error function can be expressed as:

$$E = \frac{1}{p} \sum_p \sum_k (d_{pk} - o_{pk})^2 \quad (6)$$

Where  $p$  is the index of the  $p$  training pairs of vectors,  $k$  is the index of elements in the output vector,  $d_{pk}$  is the  $k$ th element of the  $p$ th desired pattern vector, and  $o_{pk}$  is the  $k$ th element of the output vector when pattern  $p$  is presented as input to the network. Minimizing the cost function represented in equation (6) results in an updating rule to adjust the weights of the connections between neurons.

In this research study, the back-propagation neural networks (BPNN) were trained using the training sets formed by including 80 percent of data. After training, the BPNNs were tested using the testing datasets including 38 samples. There were three input and four output parameters in the experimental tests. The input variables are engine speed in rpm and the percentage of ethanol blending with the conventional gasoline fuel and engine load as percentage. The four outputs for evaluating thermal balance include useful work, heat lost through exhaust, heat lost to the cooling water and unaccounted losses as shown in Fig. 2. Therefore the input layer consisted of 3 neurons while the output layer had 4 neurons (Fig. 2).

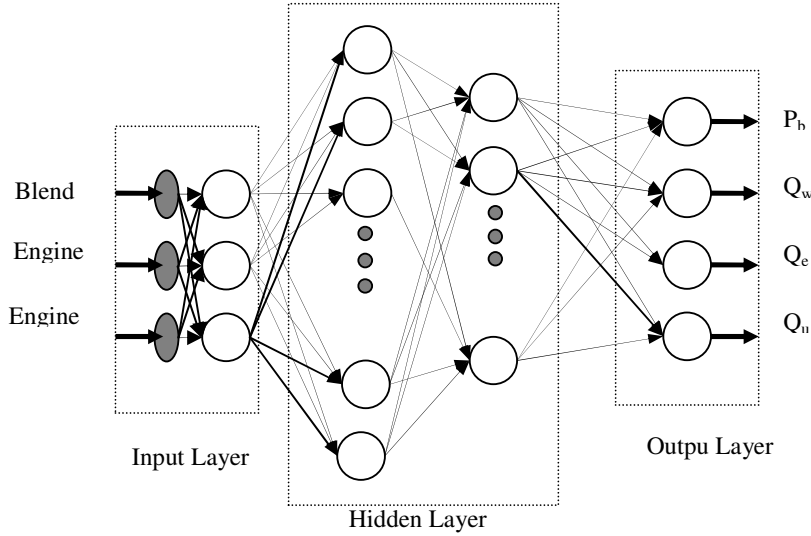


Fig. 2. Configuration of multilayer neural network for predicting engine parameters

The number of hidden layers and neurons within each layer is determined by the complexity of the problem and dataset. In this study, the number of hidden layers varied from one to two. To ensure that each input variable provides an equal contribution in the ANN, the inputs of the model were preprocessed and scaled into a common numeric range (-1,1). The activation function for hidden layer was selected to be the tangent-sigmoid transfer function which is shown in Table 4 as ‘tan’. The output of this function will fall into (-1,1) range. Furthermore, the ‘sig’ symbol in Table 4 represents log-sigmoid transfer function which squashes inputs into (0, 1) range. Linear function suited best for the output layer which is shown as ‘lin’ in Table 4. Therefore, by sig/lin as an example it is meant log-sigmoid transfer function for hidden layer and linear transfer function for the output layer. This arrangement of functions in function approximation problems or modeling is common and yields better

results. However many other networks with several functions and topologies were examined which is briefly shown in Table 4. The network topography comprises the number of neurons in the hidden layer and output layer. As depicted in Table 4, several topographies were examined but the 1 hidden layer networks e.g. [25, 4], which implies 25 neurons for the hidden layer and 4 neurons for the output layer, were preferred to 2 hidden layer ones e.g. (15,10,4), 15 neurons for the first hidden layer and 10 neurons for the second hidden layer, since the smaller size of networks is highly preferred. The training algorithms used in this paper were reported as the fastest and the most profitable for the back-propagation algorithm [22]. These fast algorithms fall into two main categories. The first category uses heuristic techniques, which were developed from an analysis of the performance of the standard steepest descent algorithm [22]. Variable learning rate (traingdx) and resilient back-propagation (trainrp) are algorithms of this category. The second category uses standard numerical optimization techniques, which include algorithms like Levenberg- Marquardt (trainlm) and Scaled Conjugate Gradient (trainscg). The function traingdx combines adaptive learning rate with momentum training. Trainrp algorithm has about the same storage requirements as traingdx but is a bit faster. The trainlm algorithm appears to be the fastest method for training moderate-sized feedforward neural networks (up to several hundred weights). Moreover, the basic idea of trainscg is to combine the model-trust region approach (used in the Levenberg-Marquardt algorithm), with the conjugate gradient approach [22].

Three criteria were selected to evaluate the networks and as a result to find the optimum one among them. The training and testing performance (MSE) was chosen to be the error criterion. The complexity and size of network is very important since the selection of hidden layers as well as neurons in the hidden layers should be well adjusted to the network inputs. A reasonably complex model will be able to handle (recognize/classify) new patterns and consequently to generalize. A very simple model will have a low performance and many patterns misclassified. Otherwise, a very complex model may well handle the exceptions present in the training set but may have poor generalization capabilities and hence over-fit the problem. So the smaller ANNs had the priority to be selected. Finally, a regression analysis between the network response (predicted values) and the corresponding targets (measured values) was performed to investigate the network response in more detail. Different training algorithms were tested and Levenberg-Marquardt (trainlm) and trainscg was selected. The computer program MATLAB (R2010a), neural network toolbox was used for ANN design.

**Table 4.** Summary of different networks evaluated to yield the criteria of network performance

Activation function	Training rule	Net Topography	Testing error	r
sig/lin	trainscg	[10,4]	$8.01 \times 10^{-1}$	0.99983
tan/lin	trainscg	[15,4]	$7.06 \times 10^{-1}$	0.99986
tan/lin	traingdx	[20,4]	0.96	0.99875
tan/lin	trainrp	[15,4]	$2.33 \times 10^{-1}$	0.99928
tan/lin	trainrp	[20,4]	$1.23 \times 10^{-1}$	0.99921
sig/lin	trainlm	[10,4]	$1.06 \times 10^{-1}$	0.99933
tan/lin	trainlm	[10,4]	$4.56 \times 10^{-2}$	0.99963
tan/lin	trainlm	[15,4]	$4.06 \times 10^{-2}$	0.99976
tan/lin	trainlm	[20,4]	$6.09 \times 10^{-2}$	0.99986
tan/lin	trainlm	[10,10,4]	$1.78 \times 10^{-1}$	0.99983
tan/lin	trainlm	[15,15,4]	$7.26 \times 10^{-2}$	0.99981
tan/lin	trainlm	[15,10,4]	$2.11 \times 10^{-1}$	0.99985
tan/lin	trainlm	[20,15,4]	$3.86 \times 10^{-2}$	0.99997
tan/lin	trainlm	[20,20,4]	$3.12 \times 10^{-2}$	0.99998
tan/lin	trainlm	[25,25,4]	$6.17 \times 10^{-2}$	0.99995

## 4 Results

### 4.1 Results of ANN

The number of hidden layers and neurons within each layer can be determined by the complexity of the problem and data set. In this study, the network was decided to consist of two hidden layers with 20 neurons. The criterion  $r$  was selected to evaluate the networks to find the optimum solution. The complexity and size of the network was also an important consideration, and therefore smaller ANNs had to be selected. A regression analysis between the network response and the corresponding targets was performed to investigate the network response in more detail. Different training algorithms were tested and Levenberg-Marquardt (trainlm) was selected. The  $r$ -values in Table 4 represent the correlation coefficient between the outputs and targets. The  $r$ -value didn't increase beyond 20 neurons in the hidden layers. Consequently the network with 20 neurons in the hidden layers would be considered satisfactory.

From all the networks trained, few ones could provide the low error condition, from which the simplest network was chosen. The results showed that the training algorithm of Back-Propagation was sufficient for predicting useful work, heat lost through exhaust, heat lost to the cooling water and unaccounted losses for different engine speeds, loads and different fuel blends ratios. The predicted versus experimental values for the experimental parameters are indicated in Fig. 3. There is a high correlation between the predicted values by the ANN model and the measured values resulted from experimental tests, which imply that the model succeeded in prediction of the engine thermal balance. It is observed in this figure that the ANN provided the best accuracy in modeling thermal balance with correlation coefficient of 0.997, 0.998, 0.996 and 0.992 for useful work, heat lost through exhaust, heat lost to the cooling water and unaccounted losses respectively. Generally, the artificial neural network offers the advantage of being fast, accurate and reliable in the prediction or approximation affairs, especially when numerical and mathematical methods fail. There is also a significant simplicity in using ANN due to its power to deal with multivariate and complicated problems. The experimental results of this study indicate that as the percentage of ethanol in the ethanol-gasoline blends increased, the percentage of useful work increased, while the other losses decreased as compared to neat gasoline fuel. This is due to the heat of vaporize of ethanol is higher than that of gasoline which makes the temperature of intake manifold lower, and decrease the peak temperature inside the cylinder, so both the exhaust gas temperature as well as the cooling water temperatures, were lower in the case of ethanol-gasoline blend operations, there was less heat loss through these channels, and as such, more useful work was available at the engine crankshaft.



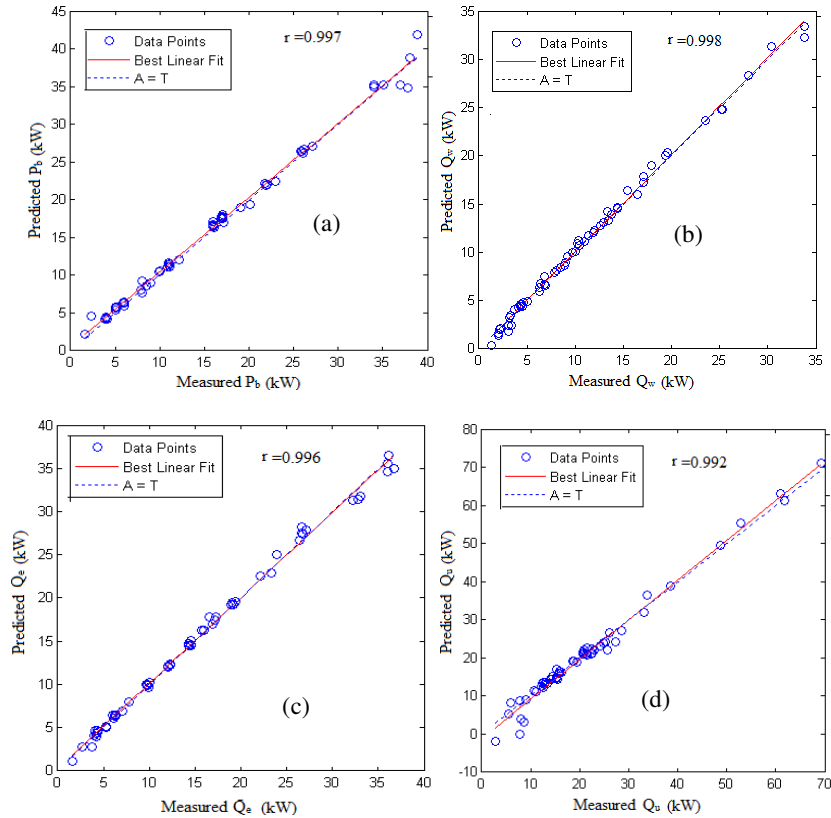


**Fig. 3.** The predicted outputs vs. the measured values, (a) useful work; (b) heat lost to the cooling water; (c) heat lost through exhaust; (d) unaccounted losses.

## 4.2 Experimental results

The thermal balance of the test engine operating on gasoline and ethanol-gasoline blends was established at different engine speed and load conditions. The thermal balance analysis and evaluation was carried out regarding useful work, heat lost to cooling water, heat lost through the exhaust and unaccounted losses. The engine thermal balance for the gasoline alone and ethanol-gasoline blends at various speeds and full load are presented in Tables 5-9. It can be seen from these tables that as the percentage of ethanol in the ethanol-gasoline blends is increased, the percentage of useful work is increased, while the heat lost to cooling water and exhaust are decreased compared to neat gasoline fuel operation. At E0, the average of the useful work was 16.76%, whereas it increased to 17.44, 18.11, 18.91 and 19.14% for E5, E10, E15 and E20 ethanol- gasoline blends respectively. Moreover, average of heat lost to cooling water was observed as 16.16, 16.30, 15.77, 15.42 and 14.71% for E0, E5, E10, E15 and E20 respectively. The average of heat lost was 23.07, 22.44, 21.91, 21.36 and 20.71% for the exhaust, and 43.51, 43.82, 44.21, 44.50 and 45.75% for unaccounted losses at E0, E5, E10, E15 and E20 ethanol- gasoline blends respectively. This is due to ethanol contains an oxygen atom in its basic form; it therefore can be treated as a partially oxidized hydrocarbon. When ethanol is added to the blended fuel, it can provide more oxygen for the combustion process and leads to more efficient combustion as compared to gasoline. The heat of vaporize of ethanol (839 kJ/kg) is higher than that of gasoline (305 kJ/kg) which makes the temperature of intake manifold lower, and decrease the peak temperature inside the cylinder, so both the exhaust gas temperature as well as the cooling water temperatures, were lower in the case of ethanol-gasoline blend operations, there was less heat loss through these channels, and as such, more useful work was available at the engine crankshaft.

**Table 5.** Data of the thermal balance for E0

Speed (rpm)	Q <sub>t</sub> (kW)	P <sub>b</sub> (kW)	Q <sub>w</sub> (kW)	Q <sub>e</sub> (kW)	Q <sub>u</sub> (kW)
1000	31.31	7.44	3.95	5.18	14.75
1500	48.85	12.13	6.35	7.76	22.61
2000	66.38	17.06	8.96	11.78	28.58
2500	83.92	22.00	11.89	16.88	33.15
3000	101.45	27.16	14.62	22.57	37.10
3500	120.24	32.00	18.54	26.15	43.55
4000	141.54	33.89	23.35	32.15	52.14
4500	162.83	37.00	27.94	36.10	61.78
5000	176.61	37.86	30.43	35.50	72.82

**Table 6.** Data of the thermal balance for E5

Speed (rpm)	Q <sub>t</sub> (kW)	P <sub>b</sub> (kW)	Q <sub>w</sub> (kW)	Q <sub>e</sub> (kW)	Q <sub>u</sub> (kW)
1000	32.79	8.08	4.47	5.34	14.90
1500	47.80	12.00	6.69	7.90	21.21
2000	64.95	16.78	9.46	12.06	26.65
2500	83.34	21.84	12.50	16.77	32.23
3000	99.27	26.90	15.53	22.90	33.95
3500	117.65	32.00	19.46	26.35	39.85
4000	138.49	34.00	23.54	32.23	48.72
4500	159.32	36.79	28.12	35.90	58.52
5000	174.03	38.13	31.59	35.06	69.25

**Table 7.** Data of the thermal balance for E10

Spee (rpm) d	Q <sub>t</sub> (kW)	P <sub>b</sub> (kW)	Q <sub>w</sub> (kW)	Q <sub>e</sub> (kW)	Q <sub>u</sub> (kW)
1000	29.75	7.47	4.32	5.34	12.63
1500	46.41	12.12	7.01	7.74	19.55
2000	63.08	17.00	10.09	11.81	24.18
2500	80.93	21.79	13.42	17.19	28.53
3000	96.40	27.00	16.70	23.06	29.65
3500	113.06	32.02	20.35	26.33	34.36
4000	134.48	34.79	24.93	31.77	42.99
4500	154.72	37.06	29.61	35.66	52.39
5000	169.00	38.89	33.16	36.01	60.94

**Table 8.** Data of the thermal balance for E15

speed (rpm)	Q <sub>t</sub> (kW)	P <sub>b</sub> (kW)	Q <sub>w</sub> (kW)	Q <sub>e</sub> (kW)	Q <sub>u</sub> (kW)
1000	28.88	7.55	4.40	5.52	11.41
1500	45.05	11.93	7.21	8.02	17.89
2000	61.22	17.12	10.25	12.32	21.52
2500	77.39	21.84	13.32	16.57	25.66
3000	94.71	27.07	17.05	23.32	27.27
3500	109.73	31.92	20.37	27.08	30.36
4000	130.52	34.06	25.26	32.77	38.43
4500	151.31	36.07	30.26	36.51	48.47
5000	165.17	38.96	33.78	35.70	56.73

**Table 9.** Data of the thermal balance for E20

speed (rpm)	$Q_t$ (kW)	$P_b$ (kW)	$Q_w$ (kW)	$Q_e$ (kW)	$Q_u$ (kW)
1000	28.11	7.62	4.5	5.54	10.45
1500	43.85	11.96	7.35	8.17	16.37
2000	59.60	16.69	10.39	12.62	19.90
2500	76.46	22.97	13.76	17.27	22.46
3000	92.20	26.98	17.39	23.59	24.24
3500	107.95	32.06	20.74	27.01	28.14
4000	127.06	35.08	25.21	33.10	33.67
4500	147.30	37.00	29.70	36.72	43.89
5000	160.80	38.10	33.77	36.11	52.82

## 5 Conclusion

An artificial neural network (ANN) was developed and trained with the collected data of this research work. The results showed that the three layer feed-forward neural network with two hidden layers ([20,20,4]) was sufficient enough in predicting thermal balance for different engine speeds, loads and different fuel blends ratios. It can be concluded that high values of regression coefficients yielded when setting a regression line for predicted and measured datasets.

The experimental results showed as the percentage of ethanol in the ethanol-gasoline blends is increased, the percentage of useful work is increased, while the heat lost to cooling water and exhaust are decreased compared to neat gasoline fuel operation.

## References

1. Graupe, D.: Principles of artificial neural networks. p. 303. In: Circuits and systems. 2nd ed. USA: World Scientific. Advanced Series( 2007)
2. Najafi, G., Ghobadian, B., Tavakoli, T., Buttsworth, D., Yusaf, T., Faizollahnejad, M.: Performance and exhaust emissions of a gasoline engine with ethanol blended gasoline fuels using artificial neural network. *Applied Energy*, 86, 630–9 (2009)
3. Yuanwang, D., Meilin, Z., Dong, X., Xiaobei, C.: An analysis for effect of cetane number on exhaust emissions from engine with the neural network. *Fuel*, 81, 1963–70 (2003)
4. Canakci, M., Ozsezen, A.N., Arcaklioglu, E., Erdil, A.: Prediction of performance and exhaust emissions of a diesel engine fueled with biodiesel produced from waste frying palm oil. *Expert Systems with Applications*, 36, 9268–9280 (2009)
5. Golcu, M., Sekmen, Y., Erduranli, P., Salman, S.: Artificial neural network based modeling of variable valve-timing in a spark ignition engine. *Applied Energy*, 81, 187–97 (2005)
6. Kalogirou, S.A.: Artificial intelligence for the modeling and control of combustion processes: a review. *Progress in Energy and Combustion Science*, 29, 515–66 (2003)
7. Czarnigowski, J.: A neural network model-based observer for idle speed control of ignition in SI engine. *Engineering Applications of Artificial Intelligence*, 23, 1–7 (2010)
8. Kalogirou, S.A.: Application of artificial neural-networks for energy systems. *Applied Energy*, 7, 17–35 (2006)
9. Prieto, M.M., Montanes, E., Menendez, O.: Power plant condenser performance forecasting using a non-fully connected ANN. *Energy*, 26, 65–79 (2001)
10. Chouai, A., Laugeier, S., Richon, D.: Modelling of thermodynamic properties using neural networks – application to refrigerants. *Fluid Phase Equilibria*, 199, 53–62 (2002)
11. Sozen, A., Arcaklioglu, E., Ozalp, M.: A new approach to thermodynamic analysis of ejector-absorption cycle: artificial neural networks. *Applied Thermal Engineering*, 23, 937–52 (2003)
12. Arcaklioglu, E.: Performance comparison of CFCs with their substitutes using artificial neural network. *Energy Research*, 28, 1113–25 (2004)
13. Ertunc, H.M, Hosoz, M.: Artificial neural network analysis of a refrigeration system with an evaporative condenser. *Applied Thermal Engineering*, 26, 627–35 (2006)
14. De Kaiadi, M., Fast, M., Assadi, M.: Development of an artificial neural network model for the steam process of a coal biomass cofired combined heat and power (CHP) plant in Sweden. *Energy*, 32, 2099–109 (2007)

15. Hannani S.K, Hessari E, Fardadi M, Jeddi M.K.: Mathematical modeling of cooking pots' thermal efficiency using a combined experimental and neural network method. *Energy*, 31, 2969–85 (2007)
16. Canakci, M., Erdil, A., Arcaklioglu, E.: Performance and exhaust emissions of a biodiesel engine. *Applied Energy*, 83, 594–605 (2006)
17. Arcaklioglu, E., Celikten I.: A diesel engine's performance and exhaust emissions. *Applied Energy* 2005;80:11–22.
18. Celik, V., Arcaklioglu, E.: Performance maps of a diesel engine. *Applied Energy*, 81, 247–59 (2005)
19. Parlak, A., Islamoglu, Y., Yasar, H., Egrisogut, A.: Application of artificial neural network to predict specific fuel consumption and exhaust temperature for a diesel engine. *Applied Thermal Engineering*, 26, 824–8 (2006)
20. Ghobadian, B., Rahimi, H., Nikbakht, A.M., Najafi, G., Yusaf, T.: Diesel engine performance and exhaust emission analysis using waste cooking biodiesel fuel with an artificial neural network. *Renewable Energy*. 34(4), 976–82, (2009)
21. Sayin, C., Ertunc, H., Hosoz, M., Kilicaslan, I., Canakci, M.: Performance and exhaust emissions of a gasoline engine using artificial neural network. *Applied Thermal Engineering*, 27, 46–54 (2007)
22. Kiani Deh Kiani M., Ghobadian B., Nikbakht A.M., Najafi G.: Application of artificial neural networks for the prediction of performance and exhaust emissions in SI engine using ethanol- gasoline blends. *Energy*, 35(1), 65-69 (2010)
23. Hakan, O., Soylemez, M.S.: Thermal balance of a LPG fuelled, four stroke SI engine with water addition. *Energy Conversion and Management*, 47, 570–581 (2006)